Morphology and spatial refractive index distribution of the retina accessed by hyperspectral quantitative phase microscopy

Álvaro Barroso[1], Steffi Ketelhut[1], Peter Heiduschka[2], Gerburg Nettels-Hackert[2], Jürgen Schnekenburger[1], Björn Kemper[1,*]

[1]Biomedical Technology Center of the Medical Faculty, University of Muenster, Mendelstr. 17, D-48149 Muenster, Germany

[2]Department of Ophthalmology, University of Muenster Medical Centre, Domagkstr. 15, D-48149 Muenster, Germany

ABSTRACT

In ophthalmologic imaging, the optical properties of the retina are essential parameters. The retina's refractive index (RI) determines the light propagation inside the tissue towards the photoreceptors and its spatial distribution reflects biophysical tissue properties. In addition, information about the RI's wavelength dependency is crucial for optical imaging, as it has to be considered, e.g., for dispersion compensation in high resolution optical coherence tomography (OCT). However, the spatial RI distribution in retinal tissue is difficult to access. We explored the capabilities of quantitative phase imaging (QPI) for RI characterization of murine retina utilizing digital holographic microscopy (DHM). Multispectral QPI was achieved by a Michelson interferometer-based DHM configuration that was combined with the light from a tunable supercontinuum laser light source.

Keywords: digital holographic microscopy, quantitative phase imaging, multi-wavelength, hyperspectral imaging, refractive index, dispersion, label-free.

1. INTRODUCTION

The optical properties of the retina are essential parameters in ophthalmologic imaging. On one hand the retina's refractive index (RI) determines the light propagation inside the tissue towards the photoreceptors. On the other hand, its spatial distribution reflects biophysical tissue properties such as (mass)density or birefringence. Moreover, the RI's wavelength dependency is crucial information for high-resolution imaging, e.g., for dispersion compensation in optical coherence tomography (OCT). However, the spatial RI distribution in retinal tissue is difficult to access.

Quantitative phase microscopy (QPM) was continuously improved during the past years for high resolution label-free quantitative imaging of unstained biological samples [1-17]. Digital holographic microscopy (DHM) [10], a variant of QPM, is an established tool for industrial non-destructive testing and a promising method for minimally invasive label-free analysis of biological specimens like living cells or dissected tissues which can be integrated modular into common research microscopes [18] for multimodal label-free imaging [19, 20]. Moreover DHM can be utilized for quantification of cell migration [21] and motility [22] as well as for analysis of living cell cultures in three-dimensional environments [23, 24]. Recently, quantitative phase imaging (QPI) has been already successfully applied for label-free quantification of cancer or inflammation in dissected tissue. Given that tissue density is directly related to changes of the spatial RI distribution, mediated tissue alterations can be analyzed from quantitative phase images (see [25] and included references). We thus explored the capabilities of QPI for RI characterization of murine retina utilizing DHM. Multi-spectral QPI was achieved by a Michelson interferometer-based DHM configuration [26] that was combined with the light from a tunable supercontinuum laser light source [27].

* bkemper@uni-muenster.de, phone: +49 251 83 52479

Optical Methods for Inspection, Characterization, and Imaging of Biomaterials IV, edited by Pietro Ferraro, Simonetta Grilli, Monika Ritsch-Marte, Christoph K. Hitzenberger, Proc. of SPIE Vol. 11060, 110600C
 · doi: 10.1117/12.2526048

For our study, we embedded unstained cryostat sections from mouse retina in phosphate buffered saline on glass carrier slides and sealed the samples with cover slips. Digital off-axis holograms of the retina sections were recorded at different wavelengths with the Michelson interferometer-based DHM setup in the near infrared spectral range that is relevant for OCT. For improved QPI, coherence induced disturbances were reduced by averaging of phase maps that were acquired at different light wavelengths. Our results demonstrate that different layers of the retina can be clearly distinguished in quantitative DHM phase contrast images. Moreover, refractive index values retrieved from the reconstructed quantitative DHM phase images were found in good agreement with previously reported values for living cells and dissected tissues.

2. MULTI-WAVELENGTH DIGITAL HOLOGRAPHIC MICROSCOPY

2.1 Experimental setup and reconstruction of quantitative phase images

The concept of the applied experimental setup for multi-wavelength modular DHM that was integrated into a common inverted microscope (AE30, Motic, Hong Kong, China) is shown in Fig. 1. Light from a tunable laser light source (SuperK EXTREME EXR-9, NKT Photonics A/S, Birkerød, Denmark) in combination with an acousto-optic tunable filter (AOTF) (Super Select nIR1, NKT Photonics A/S, Birkerød, Denmark) was coupled into a Michelson interferometer-based DHM configuration in which one of the mirrors was slightly tilted to generate digital off-axis holograms [26]. The sample was illuminated by an optical single mode fiber (SuperK FD7 PM, NKT Photonics A/S, Birkerød, Denmark) via the condenser lens of the inverted microscope. The Michelson interferometer configuration allows a robust and simplified alignment that is insensitive to changes of the object illumination and vibrations. Moreover, it can be operated with light with low coherences properties ($l_c \approx 50$ µm). A 20x microscope lens (Zeiss LD Acroplan 20x/0.4 Korr) was used for imaging the sample. Holograms could be recorded at different wavelengths λ from 640 nm to 1100 nm in steps of 0.1 nm utilizing a standard industrial camera (DKM 23UP1300, The Imaging Source, Bremen, Germany).

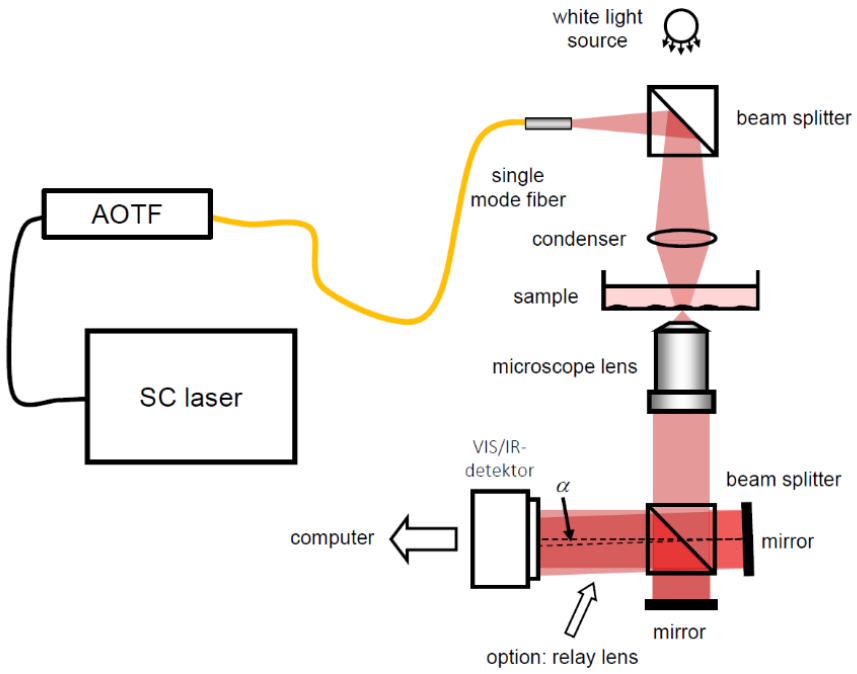

Figure 1. Concept for multi-spectral digital holographic microscopy. α: off-axis angle between object and reference wave, AOTF: Fiber coupled acousto-optic tunable filter, SC laser: fiber-coupled super continuum laser source (adapted from [27]).

The reconstruction of quantitative phase images from the acquired off-axis holograms was carried out by spatial phase shifting [2,7]. If the sample was not imaged sharply during hologram recording at different wavelength, numerical refocusing was applied [28].

2.2 Numerical reduction of coherence induced disturbances

For reduction of coherence induced disturbances, based on previous work [27, 29-32], we generated short coherence properties synthetically, utilizing the spectrally tunable supercontinuum light source. Therefore, several amplitude and phase distributions that resulted from the reconstruction of digital holograms, which are recorded separately at different laser wavelengths, were superimposed numerically.

2.3 Determination of the refractive index of buffer media

For multi-spectral refractive index retrieval of the retina, the dispersion of the embedding medium is required (see Eq. 1 in section 3.2). However, the optical properties of many physiological buffer solutions are not well characterized over a broad spectral range. We thus utilized a modified abbe refractometer (for a detailed description see [33]) to determine the refractive index's wavelength dependency of several physiological buffer solutions. The retrieved refractive index dispersion of the analyzed solutions is plotted in Fig. 2 and demonstrates that knowledge about these optical properties is essential for the hyperspectral analysis of dissected tissues.

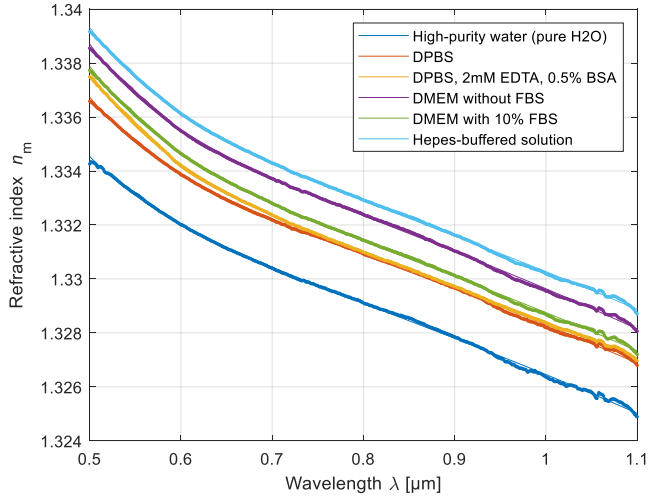

Figure 2. Refractive index dispersion retrieved in the spectral range from 500 nm to 1100 nm from measurements on different physiological buffer solutions at a temperature of 22°C. (adapted from [33]).

3. RESULTS

3.1 Multispectral quantitative phase imaging of dissected mouse retina

Fig. 3 illustrates the capabilities of multi-wavelength DHM for QPI of dissected mouse retina. Tissue sections were prepared with a specific thickness of 10 µm, fixed on conventional glass carriers, embedded in phosphate buffered saline (PBS) and covered with a cover slip for the DHM measurements. Several digital holograms were recorded at different wavelengths from λ = 800 nm to λ = 850 nm in steps of $\Delta\lambda$ = 10 nm, which are relevant in OCT-based ophthalmological imaging. Fig. 3b shows representative multi-spectral quantitative phase images of the investigated mouse retina within a field of view of 170µm x 170µm. In Fig. 3c it can be observed that coherence induced disturbances which are present in the quantitative phase images calculated from a single hologram (white arrow in Fig.3a) appear reduced by reconstruction of several quantitative phase images that were recorded at different wavelengths (Fig.3b), in combination with subsequently averaging to achieve enhanced QPI (Fig.3c). A pseudo 3D representation of the quantitative phase map of Fig. 3c is depicted in Fig. 3d.

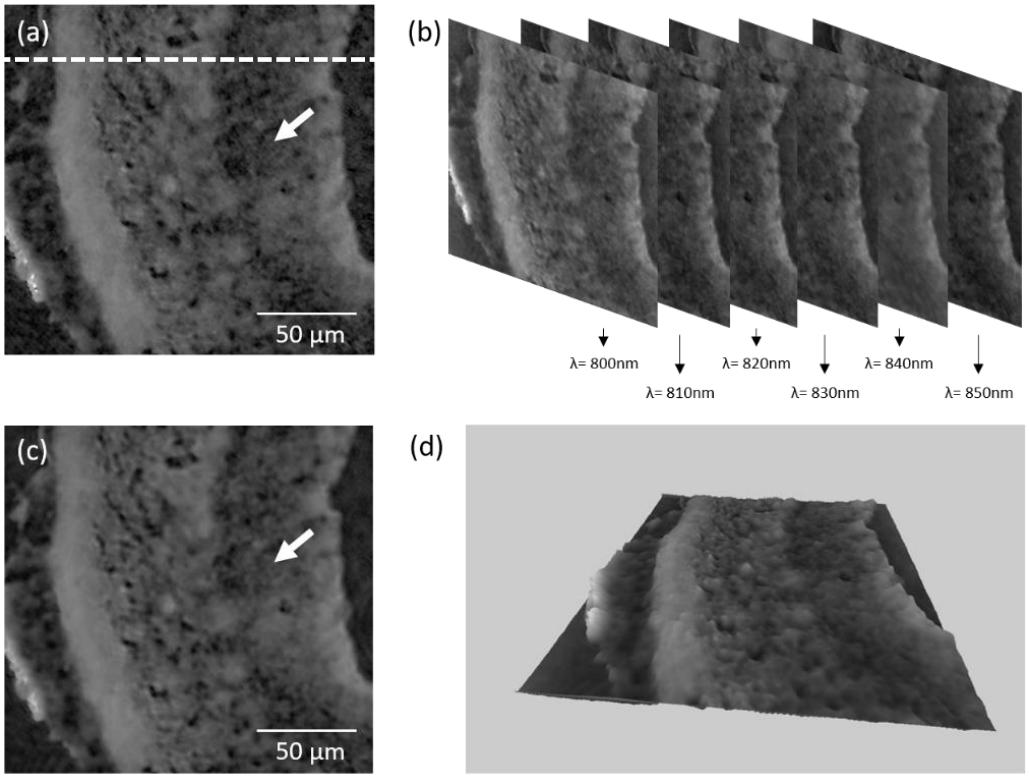

Figure 3. Quantitative phase imaging of dissected mouse retina utilizing multi-spectral digital holographic microscopy. (a) Quantitative DHM phase contrast image of a region of interest (ROI) of the retina that was obtained from a single hologram acquired at λ=800 nm. (b) Stack of quantitative phase images of the same ROI that were acquired at different wavelengths (from λ=800 nm to λ=850 nm in steps of Δλ = 10 nm). (c) Quantitative phase image resulting from averaging the quantitative phase images in (b). (d): pseudo 3D plot of the quantitative phase image in (c). The white arrows in (a) and (c) indicate the reduction of coherence induced disturbances. The dashed white line in (a) indicates the cross-section from which the spatial refractive index distributions were calculated that are plotted in Fig. 4 (adapted from [27]).

3.2 Spatially and spectrally resolved refractive index retrieval in different layers of the retina

With information about the thickness d_S of the sample, and by considering the dispersion of the embedding medium n_{medium} (see Fig. 2.), quantitative phase images $\Delta\varphi_S$ can be used to determine the integral refractive index n_S of the investigated specimen [25,34,36]:

$$n_S = n_{medium} + \frac{\lambda}{2\pi d_S}\Delta\varphi_S\,, \qquad (1)$$

where λ is the wavelength of the illuminating laser light. Fig. 4 shows the measured refractive index of the retina $n_s = n_{retina}$ along the cross section that is indicated with the dashed line in Fig. 3a [37]. The detected spatial refractive index distributions correlate with reported OCT and histology images of mouse retina. Due to the high refractive index different between consecutive cell layers, the refractive index of the ganglion cell layer (GCL), the inner nuclear layer (INL), the outer nuclear layer (ONL) and the retinal pigment epithelium (RPE) can be clearly localized. The refractive indices that are obtained for these cell layers are in well agreement with previously reported values for living cells and dissected tissues [19,20,34-36].

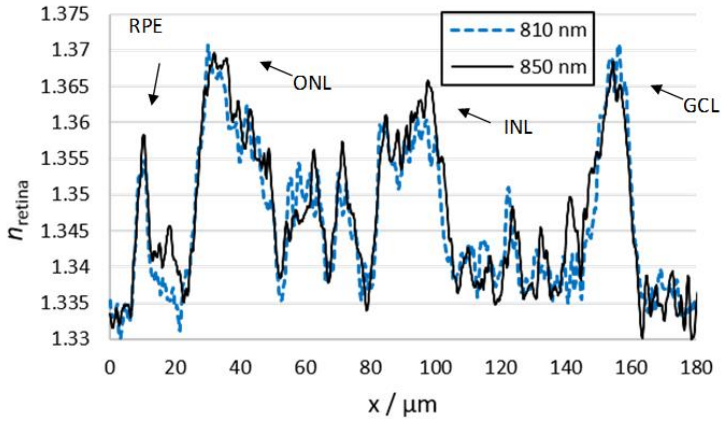

Figure 4. Representative calculated integral refractive index n_{retina} of the retina along the cross-section indicated with dashed lines in Fig. 3a for the two wavelengths λ = 810 nm and λ = 850 nm (adapted from [37]).

4. CONCLUSIONS

In conclusion, we have presented a novel approach for label-free refractive index characterization of dissected murine retina at different wavelengths utilizing multi-spectral quantitative phase imaging with DHM. Moreover, our approach can be also used to decrease coherence induced noise in DHM quantitative phase images by numerically superimposing monochromatic wave fields that were reconstructed from holograms acquired at different wavelengths. Our results retrieved from unstained cryostat mouse retina sections demonstrate that multi-spectral DHM allows the detection and quantitative analysis of the refractive index of different tissue layers. The determined refractive indices are found in good agreement with previously reported values for living cells and dissected tissues. In summary, quantitative phase imaging with multi-wavelength DHM represents a promising tool for label-free characterization of the optical properties of dissected tissues.

ACKNOWLEDGEMENTS

Funding by the European Union (Horizon 2020 Project GALAHAD, no: 732613) and support by NKT Photonics A/S, Birkerød, Denmark, is gratefully acknowledged.

REFERENCES

[1] Cuche, E. Marquet, P., Depeursinge, C., "Simultaneous amplitude contrast and quantitative phase-contrast microscopy by numerical reconstruction of Fresnel off-axis holograms," Appl. Opt. 38, 6694–7001 (1999).

[2] Carl, D., Kemper, B., Wernicke, G., von Bally, G., "Parameter optimized digital holographic microscope for high-resolution living cell analysis," Appl. Opt. 43, 6536–6544 (2004).

[3] Popescu, G., Deflores, L. P., Vaughan, J. C., Badizadegan, K., Iwai, H., Dasari, R. R., Feld, M. S., "Fourier phase microscopy for investigation of biological structure and dynamics," Opt. Lett. 29, 2503–2505 (2004).

[4] Marquet, P., Rappaz, B., Magistretti, P., Cuche, E., Emery, Y., Colomb, T., Depeursinge, C., "Digital holographic microscopy: a noninvasive contrast imaging technique allowing quantitative visualization of living cells with subwavelength axial accuracy," Opt. Lett. 30, 468-470 (2005).

[5] Mann, C. J., Yu, L. F., Lo, C. M., Kim, M. K., "High-resolution quantitative phase-contrast microscopy by digital holography," Opt. Express 13, 8693–8698 (2005).

[6] Ikeda, T., Popescu, G., Dasari, R. R., Feld, M. S., “Hilbert phase microscopy for investigating fast dynamics in transparent systems,” Opt. Lett. 30, 1165–1167 (2005).

[7] Kemper, B. Carl, D., Schnekenburger, J., Bredebusch, I., Schäfer, M., Domschke, W. von Bally, G. “Investigation of living pancreas tumor cells by digital holographic microscopy,” J. Biomed. Opt. 11, 034005 (2006).

[8] Popescu, G., Ikeda, T., Dasari, R. R., Feld, M. S., “Diffraction phase microscopy for quantifying cell structure and dynamics,” Opt. Lett., 31, 775–778 (2006).

[9] Choi, W., Fang-Yen, C., Badizadegan, K., Oh, S., Lue, N., Dasari, R. R., Feld M. S., “Tomographic phase microscopy,” Nature Meth. 4, 717–719 (2007).

[10] Kemper, B., von Bally, G., “Digital holographic microscopy for live cell applications and technical inspection,” Appl. Opt. 47, A52-A61 (2008).

[11] Debailleul, M., Georges, V., Simon, B., Morin, R., Haeberlé, O., “High resolution three-dimensional tomographic diffractive microscopy of transparent inorganic and biological samples,” Opt. Lett. 34, 79–81 (2009).

[12] Kozacki, T., Krajewski, R. Kujawinska, M. “Reconstruction of refractive-index distribution in off-axis digital holography optical diffraction tomographic system,” Opt. Express 17, 13758-13767 (2009).

[13] Shaked, N., Rinehart, M., Wax, A., "Dual-interference-channel quantitative-phase microscopy of live cell dynamics," Opt. Lett. 34, 767-769 (2009).

[14] Jang, J., Bae, C. Y., Park, J.-K., Ye, J. C., “Self-reference quantitative phase microscopy for microfluidic devices,” Opt. Lett. 35, 514–516 (2010).

[15] Shaked, N. T., Zhu, Y., Badie, N., Bursac, N., Wax A., “Reflective interferometric chamber for quantitative phase imaging of biological sample dynamics,” J. Biomed. Opt. 15, 030503 (2010).

[16] Bon, P., Maucort, G., Wattellier, B., Monneret, S., “Quadriwave lateral shearing interferometry for quantitative phase microscopy of living cells,” Opt. Express 17, 13080-13094 (2009).

[17] Ding, H., Popescu, G., “Instantaneous spatial light interference microscopy,” Opt. Express 18, 1569–1575 (2010).

[18] Kemper, B., Carl, D., Höink, A., von Bally, G., Bredebusch I., Schnekenburger, J., “Modular digital holographic microscopy system for marker free quantitative phase contrast imaging of living cells.” Proc. SPIE6191, 61910T (2006).

[19] Bettenworth, S., Lenz, P., Krausewitz, P., Brückner, M., Ketelhut, S., Domagk, D., Kemper, B., "Quantitative Stain-free and Continuous Multimodal Monitoring of Wound Healing in vitro with Digital Holographic Microscopy," PLOS ONE 9, 07317 (2014).

[20] Lenz, P., Brückner, M., Ketelhut, S., Heidemann, J., Kemper, B., Bettenworth, D., "Multimodal Quantitative Phase Imaging with Digital Holographic Microscopy accurately assesses Intestinal Inflammation and Epithelial Wound Healing," J. Vis. Exp. 13, e54460 (2016).

[21] Kemper, B., Bauwens, A., Vollmer, A., Ketelhut, S., Langehanenberg, P., Müthing, J., Karch, H., von Bally, G., “Label-free Quantitative Cell Division Monitoring of Endothelial Cells by Digital Holographic Microscopy,” J. Biomed. Opt. 15, 036009 (2010).

[22] Sridharan, S., Mir, M., Popescu, G., “Simultaneous optical measurements of cell motility and growth,” Biomed. Opt. Express 2, 2815-2820 (2011).

[23] Langehanenberg, P., Ivanova, L., Bernhardt, I., Ketelhut, S., Vollmer, A., Dirksen, D., Georgiev, G., von Bally, G., Kemper, B., “Automated 3D-Tracking of Living Cells by Digital Holographic Microscopy,“ J. Biomed. Opt. 14, 014018 (2009).

[24] Kuś, A., Dudek, M., Kemper, B., Kujawińska, M., Vollmer, A., "Tomographic phase microscopy of living 3D cell cultures," J. Biomed. Opt. 19, 046009 (2014).

[25] Bettenworth, D., Bokemeier, A., Poremba, C., Ding, N. S., Ketelhut, S., Lenz, P., Kemper, B., "Quantitative phase microscopy for evaluation of intestinal inflammation and wound healing utilizing label-free biophysical markers," Histol. Histopathol. 33, 417-432 (2018).

[26] Kemper, B., Vollmer, A., Rommel, C. E., Schnekenburger, J., von Bally, G., "Simplified approach for quantitative digital holographic phase contrast imaging of living cells," J. Biomed. Opt, 16, 026014 (2011).

[27] Barroso, Á., Ketelhut, S., Heiduschka, P., Kastl, L., Schnekenburger, J. and Kemper, B., "Hyperspectral digital holographic microscopy approach for reduction of coherence induced disturbances in quantitative phase imaging of biological specimens," Proc. SPIE 10834, 108340I (2018).

[28] Langehanenberg, P., Kemper, B., Dirksen, D., von Bally, G. "Autofocusing in digital holographic phase contrast microscopy on pure phase objects for live cell imaging," Appl. Opt. 47, D176-D182 (2008).

[29] Nomura, T., Okamura, M., Nitanai, E., Numata, T., "Image quality improvement of digital holography by superposition of reconstructed images obtained by multiple wavelengths," Appl. Opt. 47, D38-D43 (2008).

[30] Kosmeier, S., Langehanenberg, P., Przibilla, S., von Bally, G., Kemper, B., "Multi-Wavelength Digital Holographic Microscopy for High Resolution Inspection of Surfaces and Imaging of Phase Specimen," Proc. SPIE 7718, 77180T (2010).

[31] Kosmeier, S. Langehanenberg, P., von Bally, G., Kemper, B., "Reduction of parasitic interferences in digital holographic microscopy by numerically decreased coherence length," Appl. Phys. B 106,107–115 (2012).

[32] Kemper, B., Kastl, L., Schnekenburger, J., Ketelhut, S., "Multi-spectral digital holographic microscopy for enhanced quantitative phase imaging of living cells," Proc. SPIE 10503, 1050313 (2018).

[33] Barroso, Á., Radhakrishnan, R., Ketelhut, S., Schnekenburger, J., Kemper, B. "Refractive index determination of buffer solutions from visible to near-infrared spectral range for multispectral quantitative phase imaging using a calibrated Abbe refractometer," Proc. SPIE 10887, 1088729 (2019).

[34] Wang, Z., Tangella, K., Balla A., Popescu, G., "Tissue refractive index as marker of disease," J. Biomed. Opt., 16, 116017 (2011).

[35] Kastl, L., Isbach, M., Dirksen, D., Schnekenburger, Kemper, B., "Quantitative phase imaging for cell culture quality control," Cytometry Part A, 91, 470-481 (2017).

[36] Lenz, P., Bettenworth, D., Krausewitz, P., Brückner, M., Ketelhut, S., von Bally, G., Domagk, D., Kemper, B., "Digital holographic microscopy quantifies degree of inflammation in experimental colitis," Int. Biol. 5, 624-630 (2013).

[37] Barroso Peña, Á., Ketelhut, S. Heiduschka, P., Nettels-Hackert, G., Schnekenburger, J., Kemper B., "Refractive index properties of the retina accessed by multi-wavelength digital holographic microscopy," Proc. SPIE 10883, 108830X (2019).